ANL/CP--72075

DE91 011749

CRITICAL CURRENT AND FLUX PINNING BY CRYSTAL DEFECTS IN MELT-TEXTURED $YBa_2Cu_3O_x$*

(INVITED PRESENTATION)

Donglu Shi, K.C. Goretta, J.G. Chen, and A.C. Biondo

Materials Science Division
Argonne National Laboratory, Argonne, IL 60439

Invited paper presented at 2nd International Ceramic Science and Technology Congress, November 12-15, 1990, Orlando, FL

jmc

*Work supported by U.S. Department of Energy, BES-Materials Sciences under contract #W-31-109-ENG-38.

CRITICAL CURRENT AND FLUX PINNING BY CRYSTAL DEFECTS IN MELT-TEXTURED $YBa_2Cu_3O_X$

Donglu Shi, K. C. Goretta, J. G. Chen, and A. C. Biondo
Argonne National Laboratory, Argonne, IL 60439

ABSTRACT

Sintered $YBa_2Cu_3O_X$ bars 50 mm in length have been partially melted to develop highly textured microstructures. The bars exhibited large magnetic hysteresis and transport J_C values relative to conventional bulk $YBa_2Cu_3O_X$. Transmission electron microscopy observations revealed unique grain boundary features which are likely to be responsible for reduced weak-link effects. A high concentration of dislocations and some Y_2BaCuO_5 particles were present in sample matrices. After high-temperature annealing, the the intragranular J_C of the melt-textured material was considerably reduced. This reduction in J_C suggested that crystal defects such as dislocations were responsible for the stronger flux pinning in the melt-textured samples.

INTRODUCTION

The critical current density (J_C) of conventionally sintered bulk $YBa_2Cu_3O_X$ is too low for most envisioned applications (1,2). In addition, the J_C values of these forms decreases rapidly in applied magnetic fields (3). The low J_C values are attributable to effects from high crystal anisotropy, flux creep, and weak-links associated with grain boundaries. Various partial-melting methods have been found to produce $YBa_2Cu_3O_X$ with large, well-aligned grains; substantial improvements in J_C, especially in magnetic field, have resulted (3-8). Because many of the melt-textured materials carry so much current, it can be quite difficult to make accurate measurements of transport J_C

values. Magnetic hysteresis measurements and the Bean model (9) are, therefore, generally used to calculate J_c (3-8).

It has not been determined conclusively whether the large, in-field J_c values of more than 10^4 A/cm^2 at 77 K for melt-textured specimens are due to inherent improvements in intragranular J_c or to enlarged current loops associated with strong linking of grains. In this paper, experimental results of superconducting properties and microstructural characteristics are reported for melted-textured $YBa_2Cu_3O_x$ bars. Results are compared with those obtained for conventionally sintered bars. Microstructural effects on transport J_c and magnetic hysteresis are discussed.

EXPERIMENTS

All specimens were prepared from $YBa_2Cu_3O_x$ powder synthesized by solid-state reaction of Y_2O_3, $BaCO_3$, and CuO. Well-mixed powders were calcined for 4 h at 800°C in flowing oxygen at a reduced pressure of about 2.6×10^2 Pa. The powder was phase-pure by X-ray diffraction and differential thermal analysis (10). Bars were cold-pressed in a 50-mm by 7.6-mm steel die. The bars were placed on Al_2O_3 setters and sintered at 985°C in flowing oxygen.

The sintered bars were melt-textured in air in a vertical tube furnace. A thin silver coating was sputtered onto the surfaces of some bars to promote melting. The texturing heat treatment was as follows: rapid insertion into a furnace at 1150°C, hold for 0.2 h, cool in 0.1 h to 1050°C, cool to 950°C at 1°C/h. Subsequent annealing in pure oxygen at 450°C increased the oxygen content to the desired level.

Small portions of a few specimens were crushed in an agate mortar and pestle so that intragranular J_c could be examined. The specimens were first cooled in liquid nitrogen to minimize formation of dislocations during crushing. Half of the powder from a crushed melt-textured sample was annealed in air for 80 h at 880°C in an

attempt to remove dislocations. The other half was given only an oxygenation anneal. For all powders, the final anneal was at 450°C in oxygen for 4 h. Powder particle sizes were measured from scanning electron microscopy (SEM) photographs.

Small bars for property measurements were cut by diamond saw. J_C, determined with a voltage criterion of 1 μV/cm, was measured by a standard four-terminal method at 77 K. The current and voltage leads were directly soldered to the sample with pure indium. An electromagnet was used to supply a steady applied field up to 1.5 T for the J_C measurements. The magnetic hysteresis and relaxation data were taken with a commercial superconducting quantum interference device (SQUID) at various temperatures up to 5 T. Transmission electron microscopy (TEM) was performed on a Philips 420 electron microscope.

RESULTS AND DISCUSSION

Figure 1 shows the microstructure of a melt-textured (MT) sample observed by SEM. Figure 1a, a fracture surface, shows that the superconducting grains are well aligned along the ab plane and that twin boundaries are mostly normal to the grain boundaries. The concentration of Y_2BaCuO_5 (211) is low in the MT samples: back-scattered electron imaging revealed only small amounts of 211 and CuO (Fig. 1b). This is in sharp contrast to previous results for zone-melted samples in which high levels of 211 were observed (3,6-8). This microstructural difference is possibly attributable to differences in cooling conditions and silver addition. The melt-textured samples also exhibit high homogeneity as indicated by magnetization measurements: the MT sample shows a sharp superconducting transition near 90 K (Fig. 2).

Transport J_C data and characteristics of the low-angle grain boundaries have been reported elsewhere (11). Most of the grain boundaries are well aligned. The angular differences between adjacent

grains are estimated to less than 3°. Transport J_c, measured by pulsed current, has reached 4.4 x 10^4 A/cm^2 at 77 K and 1.8 T. This high J_c value is comparable to other reports (5-8) and indicates a strong correlation with the observed low-angle grain boundaries.

Magnetization (M) versus applied field (H) data were also obtained to estimate the intragranular J_c based on the Bean critical-state model. However, owing to difficulties in measuring the size of the induced current loop d, the magnetization J_c could not be accurately determined. Thus, a different approach was taken. Small parts of samples were crushed into fine powders to separate the grains. M versus H measurements were performed on these powders. To determine whether the strong pinning in the MT samples is caused by high densities of crystal defects such as dislocations, some of the powder was annealed at 880° for 80 h to remove some of the defects. For comparison, an as-sintered bar was also crushed and measured. All three samples—as melt-textured (MT), melt-textured and high-temperature annealed (MTA), and as-sintered (ST)—received identical annealing in oxygen at 450° for 4 h.

Particle sizes of the powdered samples, as estimated by SEM, exhibited distributions. Average values for each powder were between 5 and 10 μm. It is emphasized that annealing had no effect on particle size and that only relative changes in pinning strength were examined. An average particles size d was used for estimation of intragranular J_c. According to the Bean model, $J_c = 30\,\Delta M/d$, where J_c is in A/cm^2, ΔM is the magnetic hysteresis difference in emu/cm^3, and d is the particle size in cm. It is noted that the d values obtained by powdering the bulk samples are smaller than the average grain sizes of the bulk samples. This ensures that few grain boundaries are likely to exist within the particles.

Figure 3 shows the calculated J_c versus H at 10 K up to 4.7 T. The MT sample has the highest J_c (1 x 10^7 A/cm^2 at 2 T). After the high temperature anneal, J_c at the same field dropped to 4 x 10^6 A/cm^2. For the as-sintered sample, J_c is 6 x 10^5 A/cm^2 at 2 T. This consistent

decrease in J_c clearly indicates microstructural differences between samples. Figure 4 is a TEM photograph showing a high density of dislocations in the matrix of a melt-textured bar. It has been reported that stacking-fault-type defects also exist in the melt-textured samples (12). Such crystal defects have rarely been observed in conventionally sintered samples. The origins of these defects is not clear. A possible explanation is that large numbers of dislocations can be generated by a high thermal gradient during partial melting (13). Sintering temperatures, ≈ 950°C, are usually much lower than the processing temperature, ≈ 1050°C, of melt texturing.

In Fig. 5, flux pinning force density (F_p) is plotted versus reduced field $h(H/H_{c2})$. The H_{c2} value was previously estimated for the polycrystalline $YBa_2Cu_3O_x$ (14). As proposed by Fietz and Webb (15), the pinning force density $F_p(h)$ can be expressed as:

$$F_p = (H_{c2})^n (T)\, f(h),$$

where the pinning function f(h) is directly related to the specific pinning mechanisms in the system. For all type II superconductors with high upper critical field H_{c2}, pinning force density has a maximum in the F_p versus h plot. Kramer (16) suggested that F_p contains two competing parts which are related to pinning strength and the plastic shear of the flux-line lattice, respectively. The Kramer model predicts that, as a metallurgical treatment results in fewer and weaker pinning centers in the material, the peak position F_{max} shifts to lower values of h and the corresponding F_p values increase. Such a peak shift is observed, as shown in Fig. 5, which could be related to the pinning mechanism proposed by Kramer. For an MT sample, the F_p peak occurs at h = 0.012 and has the highest value of 250×10^6 TA/cm^2. After annealing the sample at 880°C for 80 h, concentrations of crystal defects such as edge dislocations and stacking faults are reduced. F_p is decreased to 120×10^6 TA/cm^2 and the peak of F_p is moved to a higher value h ≈ 0.04.

The above results suggest that the strong flux pinning effects observed in the melt-textured sample are related to the high densities of crystal defects in the sample matrices. Although it has been proposed that oxygen inhomogeneity can cause strong pinning, it should not play an important role in this study since all samples had the same oxygen treatment. The various microstructures in these samples were established through different processing methods, and processing strongly affected critical current densities.

CONCLUSIONS

A highly textured microstructure was obtained in melt-textured $YBa_2Cu_3O_X$ bars. The transport J_C in magnetic fields up to 1.5 T was greatly improved at 77 K. TEM evidence suggests that this enhancement of J_C may be connected with presence of small-angle grain boundaries. High temperature annealing resulted in considerable reduction in J_C in the melt-textured sample at 10 K. This indicates that the strong flux pinning effects are due to high densities of crystal defects in the melt-textured samples.

ACKNOWLEDGMENTS

This work was supported by the U. S. Department of Energy, Basic Energy Sciences–Materials Science and Conservation and Renewable Energy, under Contract W-31-109-ENG-38. J.G.C. is also with the Department of Materials Science and Engineering, the University of Illinois, Urbana, IL. The work of A.C.B. was done in partial fulfillment of the requirements for the Ph.D. degree at the Illinois Institute of Technology, Chicago, IL.

REFERENCES

1. M. T. Lanagan, R. B. Poeppel, J. P. Singh, D. I. Dos Santos, J. K. Lumpp, U. Balachandran, J. T. Dusek, and K. C. Goretta, "Superconducting wires," *J. Less-Common Met.* 149, 305–312 (1989).

2. N. Chen, D. Shi, and K. C. Goretta, "Influence of oxygen concentration on processing $YBa_2Cu_3O_x$," *J. Appl. Phys.* 66, 2485–2488 (1989).

3. D. Shi, H. Krishnan, J. M. Hong, D. Miller, P. J. McGinn, W. H. Chen, M. Xu, J. G. Chen, M. M. Fang, U. Welp, M. T. Lanagan, K. C. Goretta, J. T. Dusek, J. J. Picciolo, and U. Balachandran, "Transport critical current density and microstructure in extruded $YBa_2Cu_3O_x$ wires processed by zone melting," *J. Appl. Phys.* 68, 228–232 (1990).

4. S. Jin, T. H. Tiefel, R. C. Sherwood, M. E. Davis, R. B. van Dover, G. W. Kammlott, R. A. Fastnacht, and H. D. Keith, "High critical currents in Y–Ba–Cu–O superconductors," *Appl. Phys. Lett.* 52, 2074–2076 (1988).

5. K. Salama, V. Selvamanickam, L. Gao, and K. Sun, "High critical currents in bulk $YBa_2Cu_3O_x$ superconductor," *Appl. Phys. Lett.* 54, 2352–2354 (1989).

6. M. Murakami, M. Morita, K. Doi, and K. Miyamoto, "A new process with the promise of high J_c in oxide superconductors," *Jpn. J. Appl. Phys.* 28, 1189–1194 (1989).

7. P. J. McGinn, M. Black, and A. Valenzuela, "Texture processing of $YBa_2Cu_3O_{7-x}$ by Joule heat zone melting," *Physica C* 156, 57–61 (1988).

8. P. J. McGinn, W. Chen, N. Zhu, U. Balachandran, and M. T. Lanagan, "Texture processing of extruded $YBa_2Cu_3O_{6+x}$ wires by zone melting," *Physica C* 165, 480–484 (1990).

9. C. P. Bean, "Magnetization of hard superconductors," *Phys. Rev. Lett.* 8, 250–253 (1962).

10. U. Balachandran, R. B. Poeppel, J. E. Emerson, S. A. Johnson, M. T. Lanagan, C. A. Youngdahl, D. Shi, K. C. Goretta, and N. G. Eror, "Synthesis of phase-pure orthorhombic $YBa_2Cu_3O_x$ under low oxygen pressure," *Mater. Lett.* 8, 454–456 (1989).

11. D. Shi, M. M. Fang, J. Akujieze, M. Xu, J. G. Chen, and C. Segre, "High critical current density in grain-oriented bulk $YBa_2Cu_3O_x$ processed by partial-melt growth," Appl. Phys. Lett., in press.

12. Z. J. Huang, Y. Y. Xue, J. Kulik, Y. Y. Sun, and P. H. Hor, unpublished results.

13. D. Shi, J. Akujieze, and K. C. Goretta, "Processing grain-oriented bulk $YBa_2Cu_3O_x$ by partial-melt growth," Proc. 2nd World Congress on Superconductivity, September 9–13, 1990, Houston, TX, in press.

14. D. Shi, "Upper critical fields of $YBa_2Cu_3O_{7-\delta}$ with 60 K and 90 K superconductivity and the weak link effect in the system," *J. Appl. Phys.* 64, 4624–4626 (1988).

15. W. A. Fietz and W. W. Webb, "Hysteresis in superconducting alloys—temperature and field dependences of dislocation pinning in niobium alloys,"*Phys. Rev.* 178, 657–667 (1969).

16. E. J. Kramer, "Scaling laws for flux pinning in hard superconductors," *J. Appl. Phys.* 44, 1360–1370 (1973).

FIGURES

Figure 1. SEM photographs of a melt-textured bar showing (a) secondary-electron image of fracture surface and (b) back-scattered electron image of polished surface; note that little 211 is present.

Figure 2. Magnetization versus temperature at 5 G for melt-textured samples.

Figure 3. Magnetization J_c versus applied field at 10 K for the powder samples indicated.

Figure 4. TEM micrograph showing edge dislocations in a melt-textured sample; the dislocation density has been estimated to be $10^{10}/cm^2$.

Figure 5. Flux pinning force density versus reduced field (h) at 10 K for the samples indicated. The solid lines are a guide for the eye.

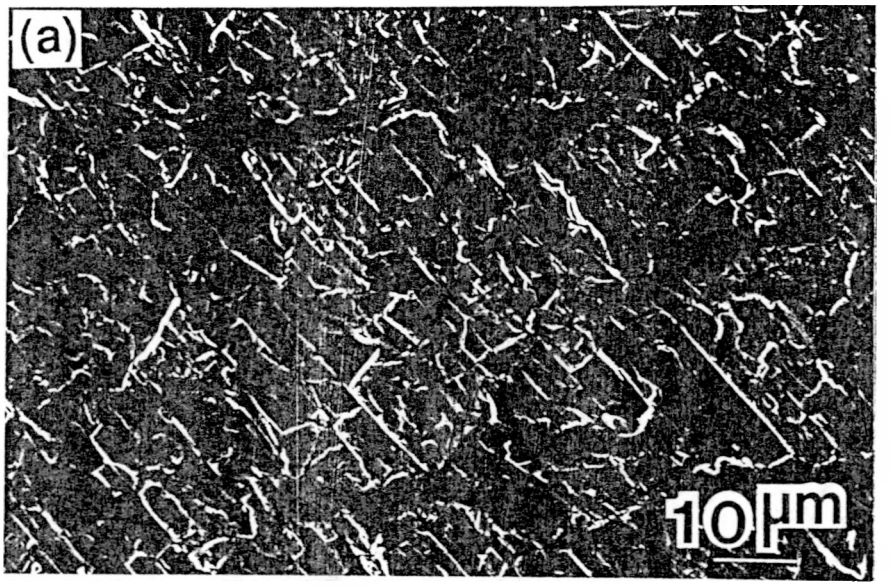

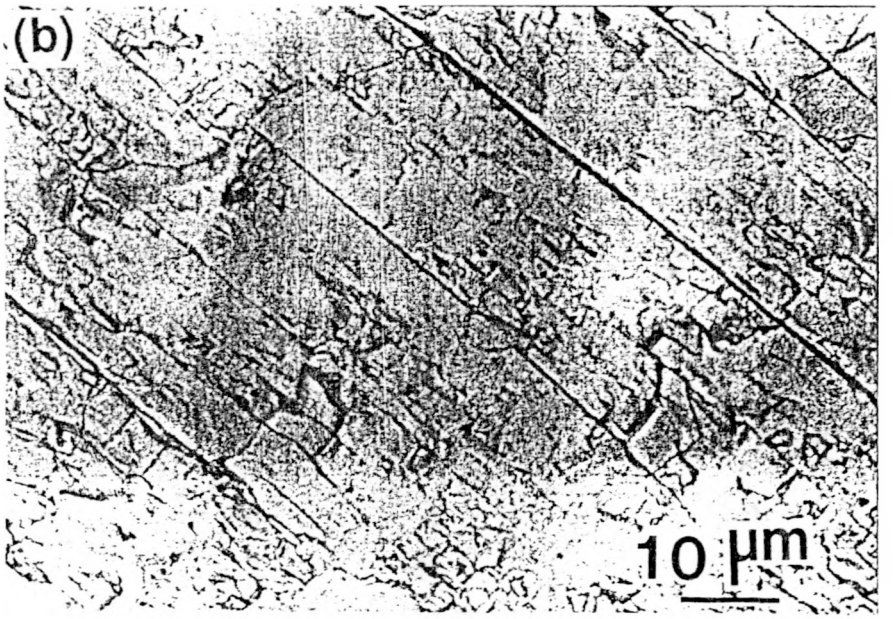

Fig 1

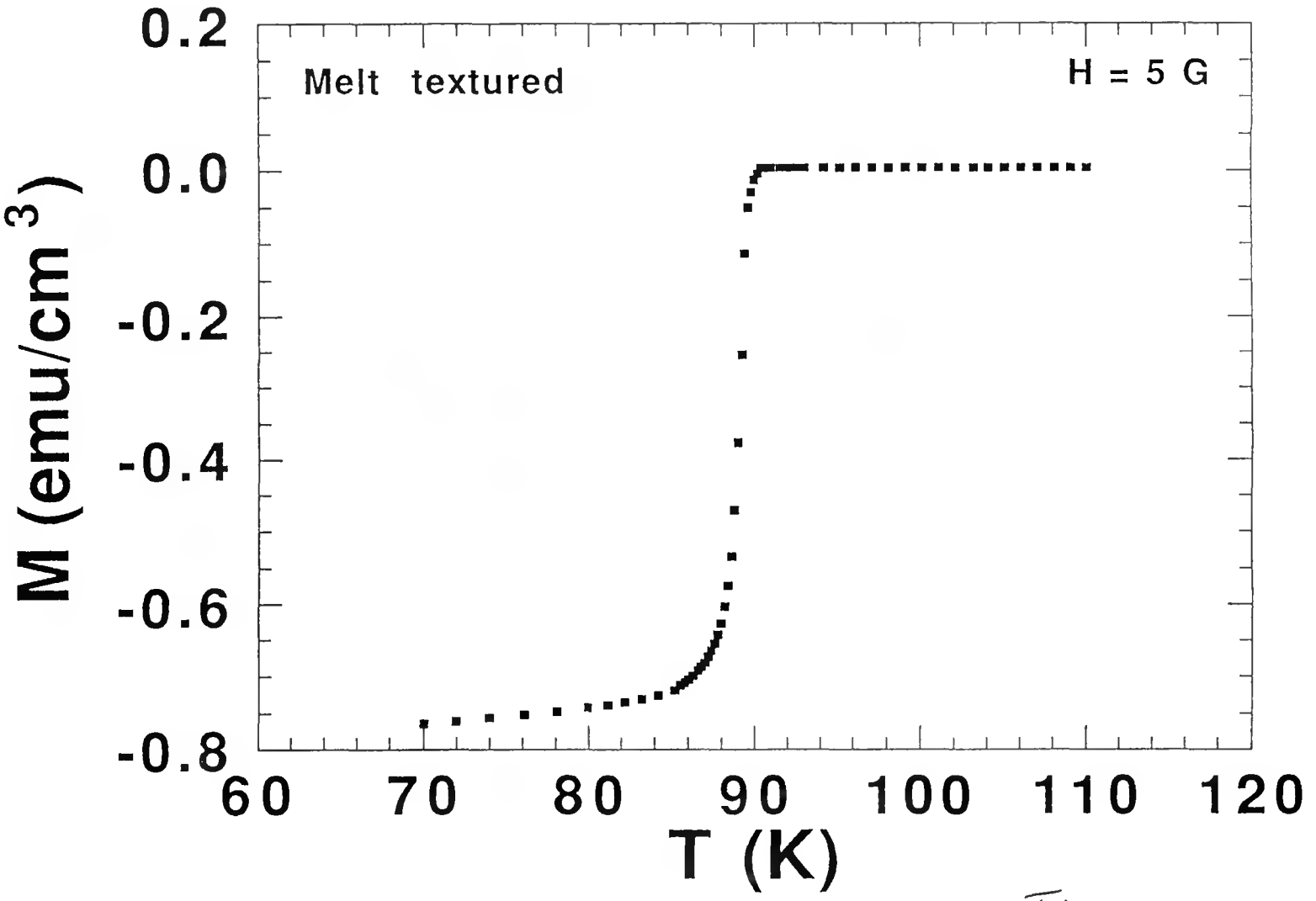
Melt textured
H = 5 G
M (emu/cm^3)
0.2
0.0
-0.2
-0.4
-0.6
-0.8
60
70
80
90
100
110
120
T (K)

Fig 2

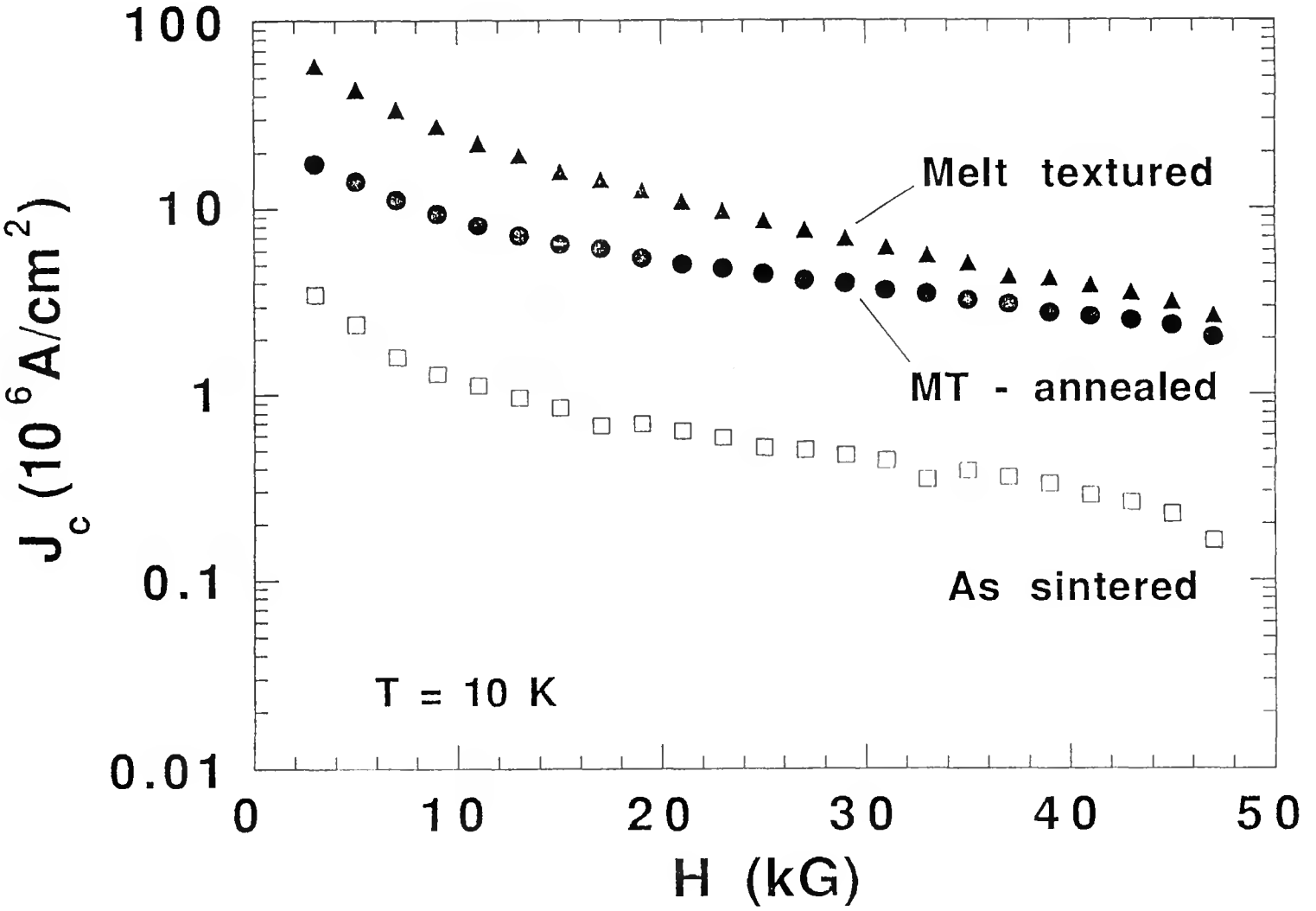
100
10
1
0.1
0.01
J_c (10^6 A/cm^2)
0
10
20
30
40
50
H (kG)
Melt textured
MT - annealed
As sintered
T = 10 K

Fig 3

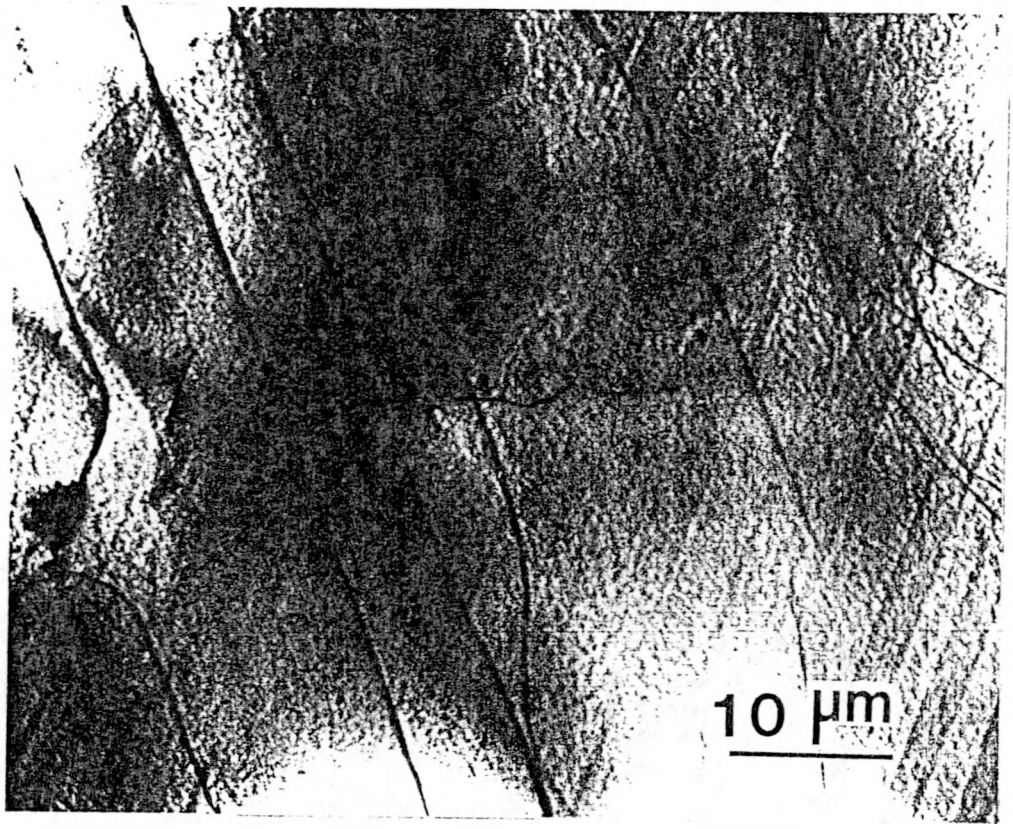

Fig 4

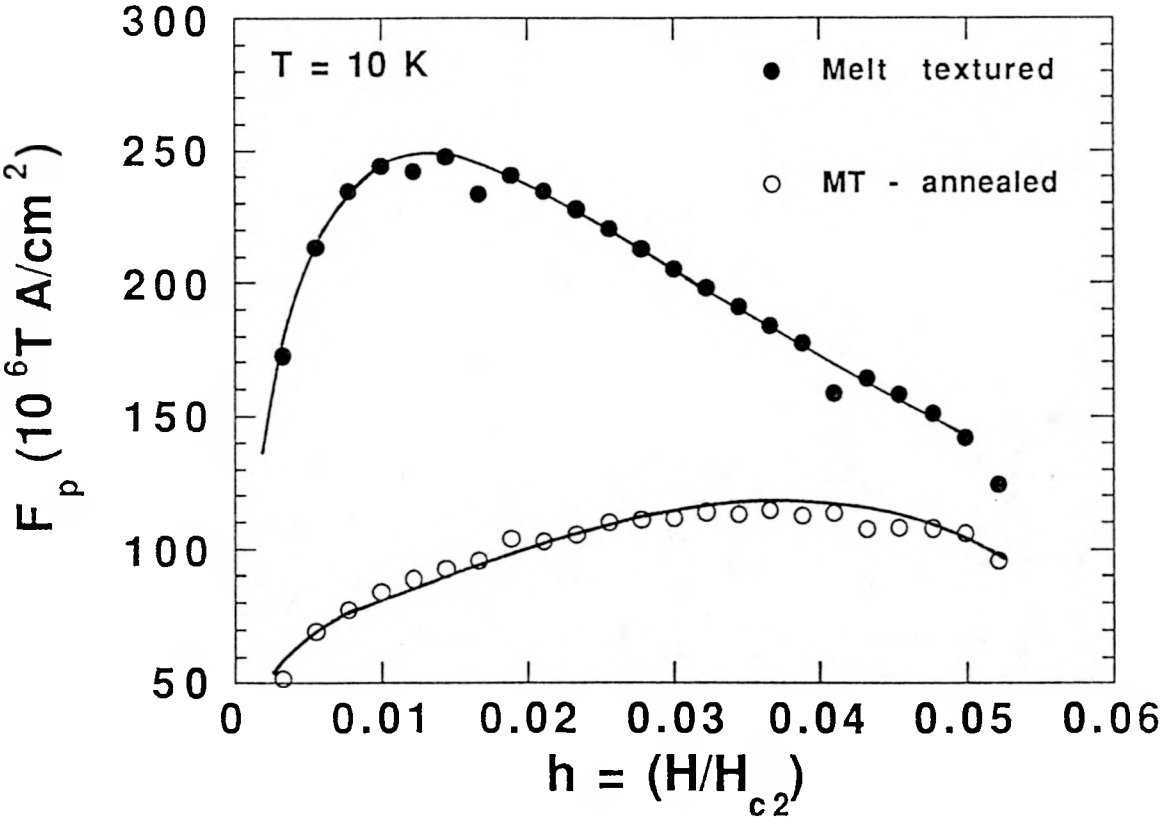
T = 10 K
Melt textured
MT - annealed
F_p (10^6T A/cm^2)
300
250
200
150
100
50
0
0.01
0.02
0.03
0.04
0.05
0.06
h = (H/H_{c2})

Fig 5